

Single-Fiber Bidirectional Transmission using 400G Coherent Digital Subcarrier Transceivers

Pablo Torres-Ferrera^{1,*}, Jacqueline Sime², Thomas Duthel², Emanuele Virgillito³, Vittorio Curri³, Roberto Gaudino³, Chris Fludger² and Antonio Napoli¹

¹ Infinera, Munich, Germany; ² Infinera, Nuremberg, Germany; ³ Politecnico di Torino, DET, Italy.

*ptorresferre@infinera.com

Abstract: We experimentally evaluate the Rayleigh Back-Scattering power penalty in a single-fiber single-wavelength bidirectional link using coherent digital subcarrier-based transceivers and verify a theoretical model in this scenario. A negligible penalty is achieved by using subcarrier-interleaving. © 2023 The Author(s)

1. Introduction

Existing solutions for front-haul and metro access networks almost entirely rely on 25G Intensity Modulation Direct-Detection (IM-DD), with the possibility to upgrade to 50G in the near future if needed [1]. Based on technology evolution and traffic requirements, mobile network operators are considering different solutions [2] for more advanced applications, such as those described in [3], which will lead to even higher capacity requirements. In this context, several multi-source agreement organizations are envisioning the deployment of coherent technology in this network segment, also to enable next generation wireless transport networks. More intelligent approaches w.r.t. backbone coherent transmission are however suggested for coherent technology deployment in the metro/access scenario. One considers the usage of simplified ZR transceivers [4] using single carrier and Polarization Multiplexing (PM)-Quadrature Phase Shift Keying (QPSK). Another proposes the broadcast of spectral slices of a coherent spectrum to different destinations to improve efficient utilization of the spectrum, i.e. the coherent Point-to-Multipoint (P2MP) technology enabled by Digital Subcarrier Multiplexing (DSCM) and using PM-16 Quadrature Amplitude Modulation (16QAM) as proposed in [5].

In this work, we propose the latter as a possible solution to enable next generation high-capacity front-hauling and we assess the case of bidirectional (BiDi) transmission with full-duplex and half-duplex (with Digital Subcarriers (DSCs) interleaved). The latter is a feature available thanks to DSCM, which allows finer control over narrow subcarriers, thus also helping in the management of the physical layer impairment of BiDi transmission.

The motivation of this work stems from the importance of transmitting bidirectionally over a single fiber. Among the benefits of this approach, the most relevant are: better usage of fiber infrastructures as fiber might be scarce; it enables low-latency systems for example by removing electronic aggregation [5]; it allows an easier management; and thanks to the interleave functionality of DSCM, it enables symmetric and asymmetric traffic and dynamic bandwidth allocation, and finally, it enables compatibility with the Passive Optical Network (PON) architecture.

In this article we report two main results: (i) that DSCM enables transmission with < 1 dB power penalty – caused by Rayleigh Back-Scattering (RB) –, for up to 20 km, with BiDi transmission of two channels at 400G both having the same central frequency and same transmitted power; and (ii) that a 200G interleaved signals suffers no penalty caused by RB. In addition, we also validate the model proposed in [6] by comparing the experimental performance against the analytical model estimations, showing high accuracy of the model.

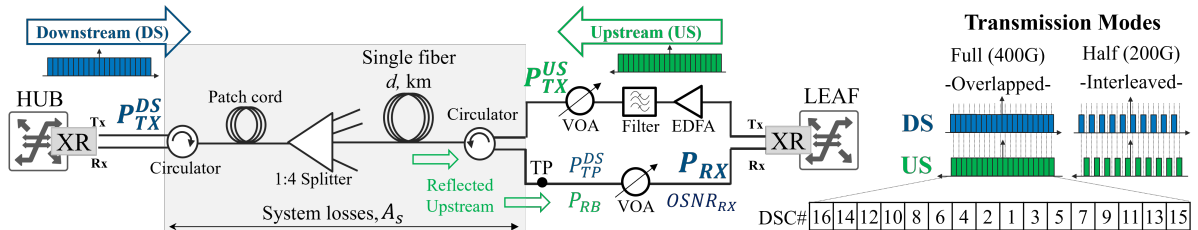


Fig. 1: Experimental setup, transmission modes, and DSC indexing

2. Experimental setup

We perform a BiDi transmission between 400G-capable (16×25 G) coherent Hub and Leaf transceivers over single-fiber using the same center frequency for both Upstream (US) and Downstream (DS). The Hub's DS channel is taken as the channel under test (CuT), while the Leaf's US channel acts as interferent. The experimental

setup is shown in Fig. 1. We fix the Hub transmitted power P_{TX}^{DS} , and we vary the Leaf's one P_{TX}^{US} , using a constant output power Erbium Doped Fiber Amplifier (EDFA) and a Variable Optical Attenuator (VOA), in order to sweep the P_{TX}^{US} to P_{TX}^{DS} ratio. This ratio is directly proportional to the amount of reflections that disturb the CuT. At the Leaf side, we vary the DS received power P_{RX} using a VOA, in order to perform RX sensitivity evaluations in different conditions. To this end, we measure the pre-FEC BER of the DS signal at the Leaf, as a function of three parameters: P_{RX} , P_{TX}^{US} , and the fiber length d . We tested two transmission modes: full and half, depicted in Fig.1. In full mode, all 16 DSCs are activated for both US and DS transmissions with an aggregated net rate of 400 Gbps per direction. In the half mode, only 8 DSCs are activated (halving the net rate), in such a way that the US and DS subcarriers are spectrally interleaved. This technique will be proven later on to eliminate the degradation caused by the reflections of the counter-propagating channel. A circulator is introduced at Hub and Leaf sides, as well as a 4 : 1 splitter, to take into account the losses and possible lumped reflections associated with these components, envisioning a point-to-multipoint scenario. The total system losses A_s are measured from the transmitter (TX) Hub port to the input of the RX Leaf VOA (test point TP). We would like to stress that, when we refer to back-to-back (BtB) configuration, we are directly connecting the Hub Tx port to the VOA located in front of the Leaf Rx port. Moreover, in BtB, the US transmission is off. Please note that the BtB case is not the same as the scenario with the complete system (i.e., including the circulators, the splitter, and active US transmission) without fiber, which in Fig.2(a) is represented as $d = 0$ km.

3. Experimental results

We perform sensitivity evaluations per DSC, for different system conditions. From pre-FEC BER versus received power (P_{RX}) curves, sensitivity is evaluated as the minimum P_{RX} delivering a certain target BER (BER_T). We use the BtB sensitivity per DSC when US is off ($P_{S,BtB}$), as the reference to calculate the experimental power penalty (ΔP) per DSC. ΔP is thus evaluated as the additional received power, with respect to $P_{S,BtB}$, needed to obtain the same BER_T in presence of US.

In Fig. 2(a) we plot the power penalty of one subcarrier, DSC#1, as a function of the P_{TX}^{US}/P_{TX}^{DS} ratio, in full mode operation. Four different fiber lengths are tested: 0, 12, 20 and 32 km. We observe that for $d = 0$ the power penalty is negligible irrespective of the P_{TX}^{US} value. This fact indicates that the reflections are caused by the fiber, and can be attributed to RB; the reflections from the rest of the elements in the system can thus be considered negligible. However, this may not be true in realistic deployed scenarios where fiber joints or bad connectors may introduce significant lumped reflections, other than RB. When considering the case where the US and DS TX powers are the same ($P_{TX}^{US}/P_{TX}^{DS} = 0$ dB), we measure a <1 dB penalty for up to 20 km distance. The penalty increases as P_{TX}^{US} is higher than P_{TX}^{DS} , since a higher power of RB reflections is generated while the power of the DS signal at the testing point TP remains constant. The power penalty increases to 2 dB for 32 km when $P_{TX}^{US} \approx P_{TX}^{DS}$. We verified similar trends for the rest of the DSCs for all fiber lengths.

In Fig. 2(b) we show the power penalty curves for three representative DSCs: one inner (DSC#1), one outer (DSC#16) and one at the middle (DSC#8), for the $d = 20$ km case. For these conditions, we show the penalty obtained operating in full and half modes. We can observe that the penalty in the half mode is negligible. Thus, the interleaving technique is effective in avoiding the degradation caused by BiDi propagation. Note that the half mode interleaving can be performed with different degrees of flexibility w.r.t. the placement of the on-off DSCs. For instance one may aggregate 2 or 4 DSCs per group, depending on the application case and instantaneous traffic conditions. Here we show just one configuration for simplicity and space limitations.

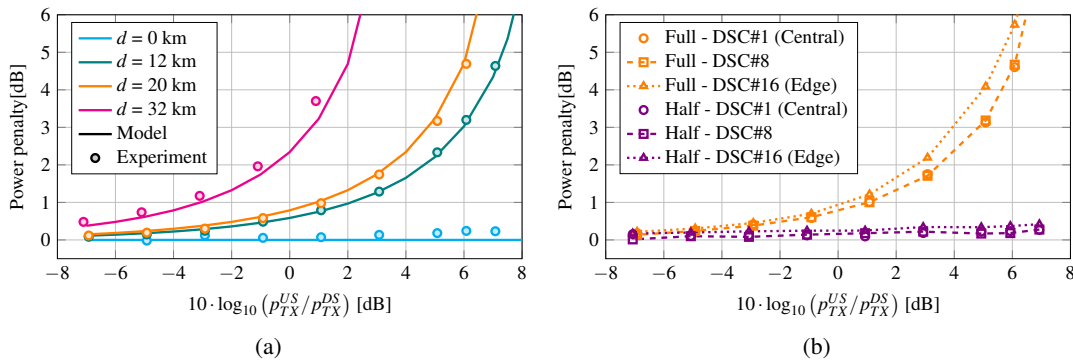


Fig. 2: Experimental power penalty versus US to DS transmitted power ratio, (a) of DSC#1 compared to the theoretical model for different fiber lengths and full mode transmission; (b) of three subcarriers for 20 km of full and half mode transmission. Each subcarrier power penalty is evaluated with respect to its own BtB sensitivity.

4. Theoretical model for full bidirectional transmission

It has been extensively demonstrated that the propagation on transparent lightpaths relying on PM coherent transceivers (TRX) can be modeled as an additive white and Gaussian noise channel (AWGN) [7], also in case of BiDi transmission [6]. So, PM TRXs can be effectively modeled by the pre-FEC bit error rate (BER) vs. the overall signal-to-noise ratio (SNR): $BER = \psi(SNR)$, where ψ is the characteristic function of the modulation format. $\psi(x) = 3/8 \cdot \text{erfc}(\sqrt{x/10})$ for the PM-16QAM that is used in our test. SNR takes into account all Gaussian noise sources impairing transmission performance: $1/SNR = 1/GSNR + 1/SNR_{TRX}$, where $GSNR$ encompasses the channel propagation degradations while SNR_{TRX} is the intrinsic transceiver degradation [8].

In the full BiDi system scenario the analyzed line impairments are the ASE noise, the RB counter-propagating channel and contributions by lumped reflections (LR), so $GSNR^{-1} = SNR_{ASE}^{-1} + SNR_{RB}^{-1} + SNR_{LR}^{-1}$, where SNR_{RB} is evaluated as follows [6]:

$$SNR_{RB} = \frac{P_{TP}^{DS}}{P_{RB}} = \frac{P_{TX}^{DS}}{A_s} \left(\frac{P_{TX}^{US} \cdot R_{RB}}{A_{c,23}^2} \right)^{-1} = \frac{P_{TX}^{DS}}{P_{TP}^{US}} \cdot \frac{A_{c,23}^2}{A_s} \left(2S\alpha_R \frac{1 - e^{-4\alpha d}}{4\alpha} \right)^{-1} \quad (1)$$

where P_{RX} and R_{RB} are the power and the equivalent reflectivity of the distributed RB, respectively. α_R (≈ 0.15 dB/km) and $S = 1.5 \cdot 10^{-3}$ are the RB field loss and the RB capture factor, respectively, defining the fiber RB reflectivity of the fiber. We remark that such reflectivity can be also experimentally characterized with a single OTDR measurement, if available. $A_{c,23}$ is the circulator loss between port 2 and 3 (≈ 0.7 dB), A_s is the total system loss, equal to 10.8, 11.6 and 15.5 dB, for fiber length of 12, 20 and 32 km. P_{TP}^{DS} is the DS power at testing point TP. Since we have not observed reflections due to the rest of the devices, the lumped losses contribution is neglected ($SNR_{LR}^{-1} = 0$).

In our setup, SNR_{ASE} is constant and equal to the measured OSNR at receiver (RX) input, $OSNR_{RX}$. The term SNR_{TRX} is dominated by the noise at the RX and specifically by the noise generated by the balanced photodetectors (BPD), so SNR_{TRX} depends on the received power. Following the approximation proposed in [9], we introduce the power dependency as follows: $SNR_{TRX} = \rho P_{RX}$, where ρ parameter accounts for the TRX noise and O/E conversion factors and losses. To compute SNR_{TRX} , we measured P_{RX} at the Leaf RX port, and we obtained ρ through fitting the BtB experimental BER vs. P_{RX} curve.

The SNR needed to achieve the BER_T is evaluated inverting the characteristic formula $\psi^{-1}(x)$ as $SNR_T = 10 \text{erfcinv}^2(8BER_T/3)$. Then, the BtB RX sensitivity at BER_T is evaluated as: $P_{S,BtB} = \rho^{-1}(SNR_T^{-1} - OSNR_{RX}^{-1})^{-1}$. The RX sensitivity at BER_T when including the RB impairments of BiDi transmission is thus $P_{S,BiDi} = \rho^{-1}(SNR_T^{-1} - OSNR_{RX}^{-1} - SNR_{RB}^{-1})^{-1}$. The power penalty ΔP due to full BiDi transmission is finally derived as Eq. 2 and compared to the power penalty measured at subcarrier DSC#1, for different fiber lengths, operating in full mode. The theoretical curves are shown in Fig. 2(a). An excellent agreement is reported.

$$\Delta P[dB] = 10 \log_{10} \left(\frac{P_{S,BiDi}}{P_{S,BtB}} \right) = 10 \log_{10} \left(\frac{SNR_T^{-1} - OSNR_{RX}^{-1}}{SNR_T^{-1} - OSNR_{RX}^{-1} - SNR_{RB}^{-1}} \right) \quad (2)$$

5. Conclusions

We report on the capability of coherent technology to enable next generation optical networks to support, e.g., upcoming beyond 5G and 6G mobile transport infrastructures. In this context, criteria such as spectrum efficiency, lower latency, simplified management, high capacity, and dynamic bandwidth allocation are essential. Our results show that a coherent transceiver using digital subcarrier multiplexing guarantees the maximum flexibility. We tested BiDi transmission showing penalty < 1 dB in full-duplex at 400G up to 20km, and no penalty in case of 200G interleaved signals, per each direction. The performance has been successfully compared against an analytical model proving its high accuracy.

Acknowledgments P. Torres-Ferrera, E. Virgillito, R. Gaudino, V. Curri and A. Napoli would like to thank the European Union' Horizon Europe research and innovation programme, GA No. 101092766 (ALLEGRO) for funding their research.

References

1. R. Bonk *et al.*, "50G-PON: The First ITU-T Higher-Speed..." *IEEE Comm. Mag.*, vol. 60, no. 3, pp. 48–54, 2022.
2. C. Castro *et al.*, "Point-to-multipoint coherent transceivers for next-generation mobile transport," in *ICTON*, 2023.
3. Z. Zhang *et al.*, "6G wireless networks: vision, requirements, ..." *IEEE Vehicular Technology Magazine*, vol. 14, 2019.
4. "Open ZR+ MSA technical specification," <https://openzrplus.org/>.
5. A. Napoli *et al.*, "Live network demonstration of point-to-multipoint coherent transmission..." in *ECOC*, 2021.
6. E. Virgillito *et al.*, "Propagation impairment in single-wavelength, single-fiber..." in *Optica APC*, 2022, p. NeTu3D.3.
7. M. Filer *et al.*, "Multi-vendor experimental validation of an open source QoT ..." *JLT*, vol. 36, no. 15, 2018.
8. T. Mano *et al.*, "Modeling transceiver ber-osnr characteristic for QoT estimation..." in *ONDM*, 2023, pp. 1–3.
9. Q. Wang *et al.*, "Accurate model to predict performance of coherent..." *Opt. Express*, no. 10, pp. 12 970–12 984.